Magnetic and thermal properties of iron-doped lead telluride

D. T. Morelli, J. P. Heremans, and C. M. Thrush
Delphi Research Laboratories, Shelby Township, Michigan 48315
(Received 28 August 2002; published 27 January 2003)

We have studied the magnetic and thermal properties of iron-doped lead telluride. Magnetic susceptibility studies reveal that the iron ion in this compound assumes the divalent state and has a solubility limit of approximately 0.13%. The lattice thermal conductivity in iron-containing samples is suppressed over a wide temperature range. This behavior is attributed to scattering of phonons between spin-orbit-split magnetic energy levels with spacing that nearly coincides with the Debye temperature of lead telluride.

DOI: 10.1103/PhysRevB.67.035206 PACS number(s): 75.50.Pp, 66.70.+f, 71.70.Ch

INTRODUCTION

Semiconducting compounds containing transition-metal (partially filled *d*-band) or lanthanide-metal (partially filled *f*-band) impurities are undergoing intense scrutiny for their interesting magnetic and electronic properties with potential application in spintronic devices. One of the best-known examples of these compounds is manganese-doped lead telluride (PbTe), a semimagnetic semiconductor[1] in which ferromagnetic coupling between Mn ions is mediated through conduction electrons via a Ruderman-Kittel-Kasuya-Yosida (RKKY)-type interaction. Subsequent studies have revealed semimagnetic semiconductor behavior in an array of II-VI (Ref. 2), III-V (Ref. 3), and group IV (Ref. 4) compounds doped with magnetic ions. The magnetic properties of PbTe containing transition-metal impurities other than Mn, however, are less well understood. A further motivation for the study of magnetic impurities in PbTe in particular is the possible enhancement of the thermoelectric properties of this compound or other semiconductors via potential reduction in lattice thermal conductivity. The focus of this work therefore was an investigation of the doping of PbTe with iron (Fe) ions and the resulting magnetic and thermal properties.

In order to gain a better understanding of the nature of transition-metal doping in PbTe, some understanding of the crystal chemistry of this compound is desirable. Lead telluride (PbTe) assumes the rocksalt (NaCl)-type structure in which the Pb and Te atoms are positioned alternately on a face-centered-cubic (fcc) lattice. As such, each Pb atom is octahedrally coordinated by Te atoms and vice versa. The bonding between Pb and Te atoms is partially ionic, and a formal charge state of 2^+ may be assigned to the Pb cation.

Looking at the transition-metal (*M*) series, all of these form tellurides at or close to the stoichiometry *M*Te; however, none of the tellurides of these elements form in the rocksalt structure. Six of them possess the NiAs structure, FeTe possesses the red PbO structure, and CuTe has its own structure.[5] Thus it is not possible to form complete solid solutions between PbTe and any *M*Te. On the other hand, the *M* atoms in all of these tellurides do have octahedral coordination so one might hope that there will be some limited solubility of these in PbTe.

In order to gain some understanding as to which transition-metal atoms may be substituted for Pb, it is useful to compare the radii of each of these ions in an octahedral environment. One might anticipate some solubility if the *M*-Te distance is close to the Pb-Te distance in PbTe, say within $\pm 5\%$. Using the procedure developed by Slack and Galginaitis for tetrahedrally coordinated transition metal elements,[6] we display in Fig. 1 the octahedral covalent radii of elements across the $3d$ series. We see that the elements Cr, Mn, Fe, Cu, and Zn fall between the dashed lines that represent the $\pm 5\%$ bounds on the radius of 1.47 Å of Pb^{2+} in PbTe. One would expect little or no solubility for Sc, Ti, V, Co, and Ni; elements beyond Cu possess a fully filled *d* shell and are not magnetic so are not considered further. As alluded to earlier, the system PbTe-MnTe has been studied in detail as this compound is a dilute magnetic semiconductor; the solubility of Mn in the PbTe lattice is quite large,[7] as high as 30%. The solubility of Cr in PbTe appears to be less than a few percent.[8] The case of Fe in PbTe is poorly understood; Andrianov *et al.*[9] found a solubility of less than 1% with the formation of clusters of ferromagnetic iron at higher concentrations.

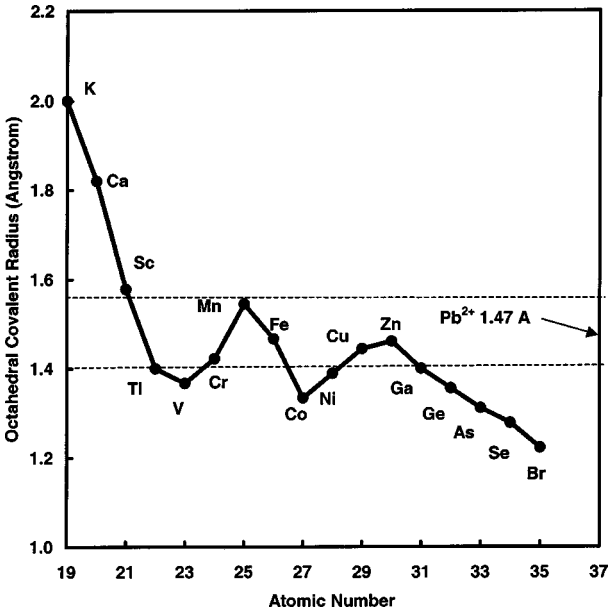

FIG. 1. Covalent octahedral radius of ions of the first-row transition-metal series in the divalent state. Region between the dashed lines represents a radius range of $\pm 5\%$ that of Pb^{2+} in PbTe.

TABLE I. Samples used in this study. Nominal composition is that determined from relative quantities of starting material; paramagnetic impurity concentration is the concentration of the transition-metal impurity in the paramagnetic state as determined from analysis of magnetization data. *A*, *B*, and *C* represent the coefficients of point defect, umklapp, and magnetic phonon scattering, respectively, ω_0 is the resonant frequency for magnetic scattering, and *L* is the crystallite size.

Nominal composition	Paramagnetic impurity concentration (at. %)	L (μm)	A (s^3)	B ($s\,K^{-1}$)	C (s^{-1})	ω_0 (s^{-1})
PbTe		8	1.3×10^{-41}	9.85×10^{-18}	0	
$Pb_{0.998}Mn_{0.002}Te$	0.16	7	3.7×10^{-41}	9.85×10^{-18}	0	
$Pb_{0.9992}Fe_{0.0008}Te$	0.07	7	2.2×10^{-41}	9.85×10^{-18}	1.5×10^{12}	1.3×10^{13}
$Pb_{0.9985}Fe_{0.0015}Te$	0.13	3	3.7×10^{-41}	9.85×10^{-18}	4×10^{12}	1.3×10^{13}
$Pb_{0.998}Fe_{0.002}Te$	0.11					
$Pb_{0.995}Fe_{0.005}Te$	0.13					

EXPERIMENT

Samples were fabricated by adding equal molar amounts of pure iron powder and Te chips to pure PbTe. This mixture was placed in a quartz ampoule, evacuated to 10^{-6} Torr, and sealed. The ampoule was lowered into a furnace, heated to 1000 °C and held at this temperature overnight. The ampoule was then removed and quenched in a bath of cold water. The resultant boule was sectioned for x-ray, magnetic, and thermal conductivity measurements. For comparison, a pure PbTe sample was melted and quenched using the same method as that used for the alloyed samples.

In order to determine the amount of magnetic impurity present and its magnetic state we have performed magnetization measurements using a Quantum Design magnetometer. By measuring the magnetization over a wide range in both temperature (5–300 K) and magnetic field (0–5.5 T), it is possible to determine the charge state and concentration of the magnetic ion.

Thermal conductivity measurements were carried out over the temperature range 4–320 K using a steady-state technique. In this method one end of a parallelepiped or cylindrically shaped sample is glued to the cold tip of a cryostat using silver paint. The other, free, end of the sample is equipped with a small metal-film heater. A differential Chromel-constantan thermocouple is glued to two points along the length of the sample using an electrically insulating epoxy. When the heater is energized with current, Joule heat flows down the sample and a resulting temperature difference along the length of the sample is established from which the thermal conductivity can be determined.

RESULTS AND DISCUSSION

Table I displays the samples used in this study. These include pure PbTe as well as PbTe doped with 0.08, 0.15, 0.2, and 0.5 at. % Fe, and 0.2 at. % Mn. These are nominal concentrations of impurity determined from the amount of transition metal initially added to the mixture before reacting. Impurity concentrations were also determined from analysis of magnetization data for samples possessing a magnetic moment (column 2). In the case of Fe, the impurity enters the lattice both substitutionally (as Fe^{2+}) and in clusters (ferromagnetic metallic iron), and an analysis of the magnetization data permits a determination of the concentration of both types. This will be discussed in detail in the following.

Magnetization Measurements

The magnetization of the pure PbTe sample was found to be diamagnetic, linear in field, and temperature independent over the entire field and temperature ranges. Figure 2 shows the magnetization as a function of applied field at 300 K for samples containing nominally 0.5, 0.2, and 0.15 at. % Fe. The magnetization of these samples is characterized by a rapidly rising portion (a ferromagnetic component) and a portion linear in field with negative slope (a combination of paramagnetic and diamagnetic terms with the diamagnetic term dominating). Clearly as the iron concentration is reduced from 0.5 at. % the ferromagnetic component is diminished, essentially vanishing for the 0.15 at. % Fe sample. In order to analyze these results, we write the magnetization of these samples as follows:

$$M = M_{\mathrm{dia}} + M_{\mathrm{para}} + M_{\mathrm{ferro}}. \tag{1}$$

Here M_{dia} is a diamagnetic background contribution, which is assumed linear in applied magnetic field and temperature independent. M_{para} is a paramagnetic contribution that, as we will show later, arises from Fe^{2+} ions substituted for Pb in the PbTe lattice. This contribution follows a Brillouin function with applied field and temperature. M_{ferro} is a ferromagnetic contribution, which presumably arises from clusters of Fe atoms; it is temperature independent and saturates at very low field ($\sim$1 T). The different temperature and field dependencies of these quantities allows for their separation. From the high-field slope at room temperature we determine the combined paramagnetic and diamagnetic contributions; subtracting this quantity from the measured data yields the ferromagnetic background term. The combined diamagnetic and paramagnetic term is then determined as a function of

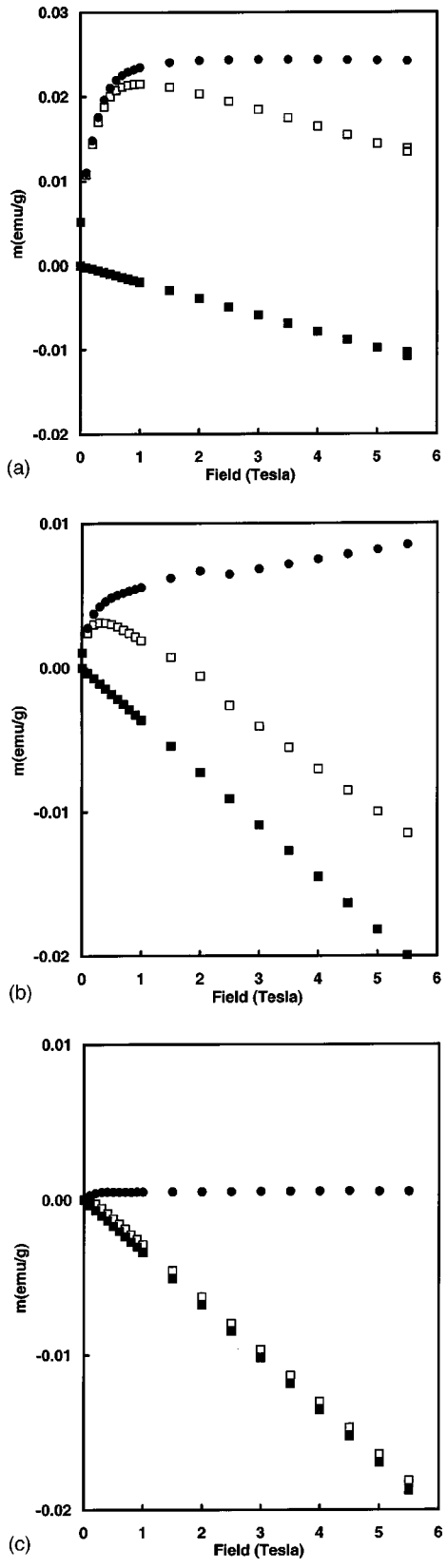

FIG. 2. Room-temperature magnetization of $Pb_{1-x}Fe_xTe$ samples (a) $x=0.005$; (b) $x=0.002$; (c) $x=0.0015$. The open squares are the experimental data; the closed squares represent the combined diamagnetic/paramagnetic term, and the closed circles the ferromagnetic term.

temperature at 0.5 T by subtracting this ferromagnetic term. This term is expected to behave as

$$M_{\text{dia,para}}=M_{\text{dia}}+M_{\text{para}}=A+B/T. \tag{2}$$

Here A is negative and represents the diamagnetic background. Thus a plot of MT vs T will yield a straight line of slope A, representing the diamagnetic contribution M_{dia}. Finally the paramagnetic contribution M_{para} is extracted by subtracting both the ferromagnetic and diamagnetic contributions from the data; the resulting paramagnetic component for the samples containing 0.08 and 0.15 at.% iron are shown in Figs. 3(a) and 3(b), respectively. We see that this paramagnetic component, in emu/mol Fe, is essentially identical for these two samples. In fact, even in samples that have a ferromagnetic component (namely, the 0.2 and 0.5 at.% samples shown in Fig. 2), the paramagnetic portion derived by the above analysis is identical to the samples with lower iron concentrations. For comparison, the paramagnetic portion of the magnetization of the 0.2 at.% Mn-doped sample (which incidentally showed no ferromagnetic features), determined in the same fashion, is shown in Fig. 3(c).

Further analysis of the paramagnetic term may be performed. Looking at the data at 5 K, we see that the paramagnetic term is linear at low field and begins to saturate at high field; this is a Brillouin function with the saturation field determined by the spin state of the magnetic ion. Accordingly, the magnetization as a function of field and temperature is given by[10]

$$M=N_A g J \mu_B B_J(x), \tag{3}$$

where

$$B_J(x)=\frac{2J+1}{2J}\coth\left[\frac{(2J+1)x}{2J}\right]-\frac{1}{2J}\coth\left[\frac{x}{2J}\right]. \tag{4}$$

Here $J=L+S$ is the total quantum number of the magnetic ion and consists of the sum of its spin (S) and orbital (L) angular momentum contributions. The g factor is given by[10]

$$g=\frac{3}{2}+\frac{1}{2}\left[\frac{S(S+1)-L(L+1)}{J(J+1)}\right] \tag{5}$$

and

$$x\equiv g J \mu_B/k_B T. \tag{6}$$

As is well known[10] for transition-metal ions, the crystal field of neighboring ions causes a quenching of the orbital moment, and the magnetization behaves very nearly as though $L=0$. The total angular momentum J is then approximately equal to the total spin angular momentum S; for the Fe^{2+} state with four unpaired spins, we expect $S=2$. As can be seen in Fig. 3, the magnetization of Fe^{2+} in PbTe is consistent with this scenario. The concentration of Fe^{2+} derived from these data saturates at approximately 0.13 at.%; see Table I. This sets the solubility limit for Fe substituting for Pb in PbTe. The data for the Mn-doped sample, Fig. 3(c) can be similarly fitted using a Brillouin function with $J=S=\frac{5}{2}$, consistent with the ${}^6S_{5/2}$, $L=0$ state of the divalent Mn^{2+} ion.

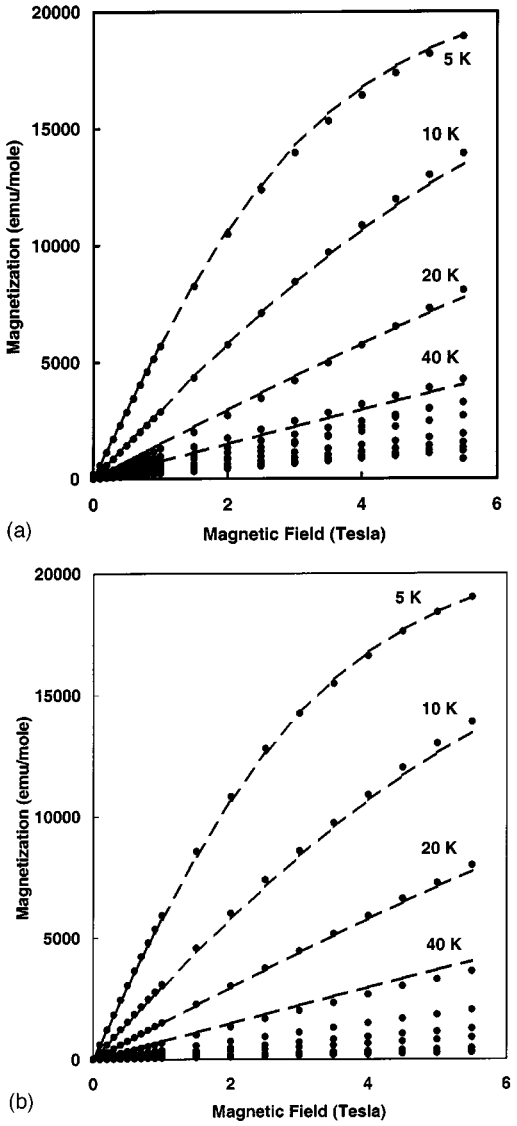

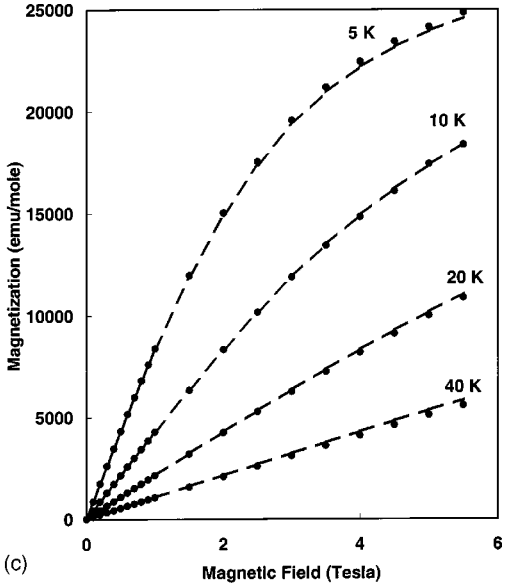

FIG. 3. Paramagnetic portion of the magnetization for two $Pb_{1-x}Fe_xTe$ samples. (a) $x=0.0008$; (b) $x=0.0015$. The dashed lines are a fit to the data using a Brillouin function with $J=2$. The only adjustable parameter is the concentration of Fe atoms in the $+2$ state. For comparison the paramagnetic magnetization of a sample containing 0.2 at. % Mn is shown in (c) along with a fit (dashed lines) to a Brillouin function with $J=\frac{5}{2}$ (Mn^{2+}). The unfit data in (a) and (b) were taken at 60, 80, 100, 150, 200, 250, and 300 K, respectively, but were not fit due to the smallness of the paramagnetic signal.

Thermal conductivity

Figure 4 shows the lattice thermal conductivity of pure PbTe and PbTe doped with the various levels of Mn and Fe. The electronic contribution to the thermal conductivity is negligible and thus these curves represent the lattice thermal conductivity of these samples. We see that for comparable concentrations, the scattering by Fe impurities is much stronger than that by Mn impurities. While a reduction in thermal conductivity due to mass fluctuation scattering is expected in doped samples, one expects little difference in this effect for Mn and Fe since these impurities have nearly the same mass and atom size. Clearly the reduction in thermal conductivity is dependent on the magnetic state of the impurity ion.

Previous studies on electrically insulating solids[11–14] have shown that a reduction in thermal conductivity can occur when the magnetic impurity ion possesses magnetic energy levels with spacings comparable to the energy of a heat-carrying phonon. A phonon having an energy equal to the difference between two neighboring magnetic levels can promote an electron from the lower to the higher energy level and the absorbed in the process. When the excited electron relaxes back to the lower-energy state, a phonon is emitted incoherently, constituting a scattering process. As others have done, we can model this process using a resonant-type scattering term to represent the magnetic scattering by the impurity. In order for this effect to occur over a wide temperature range, we need to have magnetic energy levels with spacings near the Debye temperature. For transition-metal ions, the crystal-field effect is large and causes splittings of several thousand kelvins; however, spin-orbit coupling causes a perturbation that can produce splitting on the order of a hundred kelvins. This is what gives rise to the strong phonon scattering of Fe^{2+} in MgO.[11] Given that the Fe ion in the same crystal-field environment as in MgO, a similar effect should occur in PbTe with Fe doping. In the case of the transition-metal impurities, Mn^{2+} has a half-filled d shell, $L=0$, and we expect no magnetic scattering. The case of Fe^{2+} in an octahedral field is well known[15] and has been treated using crystal-field theory. The free-ion Fe^{2+} ^5D term is split by the octahedral crystal field into an orbital triplet ($^5T_{2g}$) and a higher orbital doublet (^5E_g). The magnitude of this splitting is on the order of the crystal-field parameter

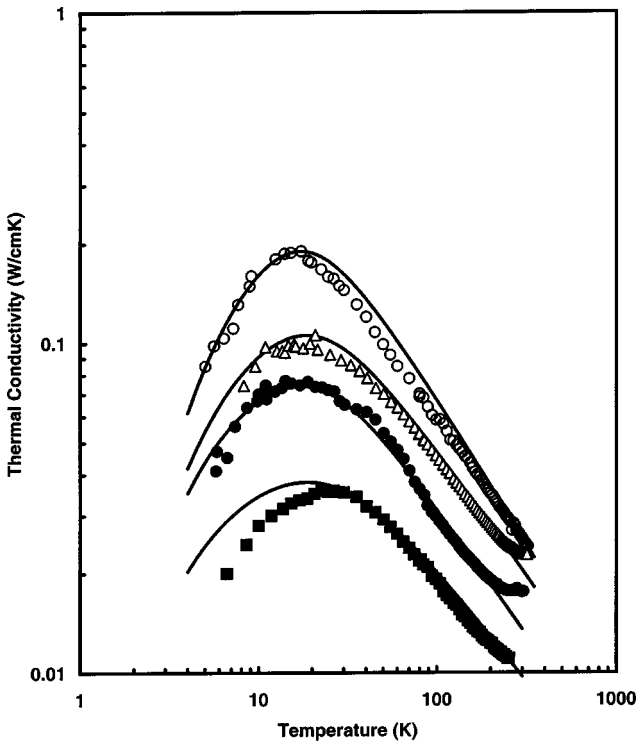

FIG. 4. Thermal conductivity of PbTe containing Fe and Mn impurity ions at various concentrations and some fits to the data (solid lines) using the procedure described in the text. Open circles, pure PbTe; open triangles, PbTe+0.2 at. % Mn; closed circles, PbTe+0.08 at. % Fe; closed squares, PbTe+0.15 at. % Fe.

$\Delta \sim 2.0\times10^{-19}$ J. This corresponds to a temperature of $T=\Delta/k_B \approx 15\,000$ K, far above the energy of a heat-carrying phonon at room temperature. Spin-orbit coupling, however, further splits the lower level into three levels at energies $+3\lambda$, $+\lambda$, and -3λ, where $\lambda \sim -2\times10^{-21}$ J is the spin-orbit coupling parameter. Thus the splitting between the lowest state and the first excited state is predicted to be $2\lambda=4\times10^{-21}$ J$\sim$300 K. Experimentally, infrared absorption measurements of Fe-doped MgO reveal[16] a peak at 2.1×10^{-21} J (157 K).

We use the Debye model of thermal conductivity in order to quantitatively account for our observed results. In this model the thermal conductivity may be expressed as

$$\kappa_L = \frac{k_B}{2\pi^2\nu}\left(\frac{k_B T}{\hbar}\right)^3 \int_0^{\Theta_D/T} \frac{x^4 e^x}{\tau_C^{-1}(e^x-1)^2}\,dx, \qquad (7)$$

where $x=\hbar\omega/k_B T$ is dimensionless, ω is the phonon frequency, k_B is the Boltzmann constant, $\hbar$ is the Planck constant, $\Theta_D=105$ K is the Debye temperature, $\nu=1181$ m s^{-1} is the average velocity of sound, and τ_C is the phonon scattering relaxation time. The phonon scattering relaxation rate τ_C^{-1} can be written as

$$\tau_C^{-1} = \frac{\nu}{L} + A\omega^4 + B\omega^2 T \exp\left(-\frac{\Theta_D}{3T}\right) + \frac{C\omega^4}{(\omega^2-\omega_0^2)^2}, \qquad (8)$$

where L is the grain size, and the coefficients A and C are the fitting parameters. The terms in Eq. (11) represent the grain-boundary scattering, point-defect scattering, phonon-phonon umklapp scattering, and magnetic phonon scattering, respectively. The quantity ω_0 represents the magnetic energy level spacing, which scatters phonons. For the umklapp scattering rate coefficient B we use the expression given by Slack and Galginaitis.[6]

$$B = \frac{\hbar\gamma^2}{M\nu^2\Theta}, \qquad (9)$$

where $\gamma \approx 2$ is the Grüneisen constant and M is the average atomic mass.

The fits to the thermal conductivity using these expressions are shown in Fig. 4 for pure PbTe and PbTe doped with 0.2 at. % Mn, 0.07 at. % Fe, and 0.15 at. % Fe. The procedure we followed to produce these fits was to (a) first fit the data on the pure sample using $C=0$ and A and L as adjustable parameters; (b) fit the data on the Mn-doped sample by altering only the magnitude of the point-defect scattering rate coefficient A from the value for the pure sample; and (c) fit the data for the Fe-doped sample using the same parameters as those for the Mn-doped sample but allowing C and ω_0 to vary and scaling A with the impurity-ion concentration. The resulting values of the parameters so derived are shown in Table I. First, we note that in order to fit the data on the pure sample we require a grain size on the order of a few micrometers; this is consistent with that which we observed in optical micrographs of these samples. Second, the pure sample also requires a nonzero value for the point-defect scattering parameter A; in fact, the value derived here could arise from on the order of 0.05 at. % vacancies, not an unusually high number for the type of boule growth used here. For the case of Mn substitution for Pb we can estimate the expected value of the point-defect scattering parameter due to the mass and size difference of Mn and Pb using the following expression:[17]

$$A = \frac{cV_A}{4\pi\nu^3}\left(\frac{M_{\mathrm{Mn}}-M_{\mathrm{Pb}}}{M_{\mathrm{Pb}}} + 2\gamma\alpha\right)^2, \qquad (10)$$

where $c \approx 0.002$ is the relative concentration of Mn ions, $V_A \approx 3.36\times10^{-29}$ m^3 the volume per atom, $M_{\mathrm{Mn}}=54.94$ the atomic mass of Mn, $M_{\mathrm{Pb}}=207.2$ the atomic mass of Pb, $\gamma \approx 2$ the Grüneisen constant, and $\alpha \approx 0.15$ the relative difference in the atomic volume of divalent Pb and Mn ions. This yields the value $A \approx 7\times10^{-42}$ s^3, in reasonably good agreement with the increase in the value of A ($\approx 2.4\times10^{-41}$ s^3) for the Mn-doped sample over that of the pure PbTe sample.

Finally, the value of ω_0 required for the resonant scattering of phonons in the iron-doped samples corresponds to a temperature of 97 K. This is near the energy spacing of 157 K determined from infrared absorption measurements on Fe-doped MgO and nearly coincides with the Debye temperature of PbTe. We thus believe that the strong depression we observe in the thermal conductivity of Fe-doped PbTe over the range 10–300 K arises due to this rather fortuitous coincidence of the spin-orbit-split energy level spacing with the Debye temperature of PbTe.

In conclusion, we have studied the magnetic and thermal properties of iron-doped lead telluride. We find that the solubility of iron in PbTe is 0.13% and the Fe ion assumes a divalent state. The lattice thermal conductivity of Fe-doped samples is suppressed by magnetic scattering of phonons, which is particularly strong due to the coincidence of the characteristic energy of the magnetic scattering with the Debye temperature of PbTe.

ACKNOWLEDGMENT

The authors would like to thank Dr. Dale Partin for helpful discussions.

[1] T. Story, R. R. Galazka, R. B. Frankel, and P. A. Wolff, Phys. Rev. Lett. **56**, 777 (1986).
[2] W. M. Becker, in *Semiconductors and Semimetals*, edited by J. K. Furdyna and J. Kossut (Academic, Boston, 1988), Vol. 25, p. 35.
[3] H. Ohno, A. Shen, F. Matsukura, A. Oiwa, A. Endo, S. Katsumoto, and Y. Iye, Appl. Phys. Lett. **69**, 363 (1996).
[4] S. Cho, S. Choi, S. C. Hong, Y. Kim, J. B. Ketterson, B.-J. Kim, and Y. C. Kim, Phys. Rev. B **66**, 033303 (2002).
[5] R. W. G. Wycoff, *Crystal Structures* (Interscience, New York, 1948).
[6] G. A. Slack and S. Galginaitis, Phys. Rev. A **133**, A253 (1964).
[7] Z. Korczak and M. Subotowicz, Phys. Status Solidi **77A**, 497 (1983).
[8] B. A. Akimov, N. A. Lvova, and L. I. Ryabova, Phys. Rev. B **58**, 10 430 (1998).
[9] D. G. Andrianov, S. A. Belokon', V. M. Lakeenkov, O. V. Pelevin, A. S. Savelév, V. I. Fistul', and G. P. Tsiskarishvili, Fiz. Tekh. Poluprovodn. 14, 175 (1980) [Sov. Phys. Semicond. **14**, 102 (1980)].
[10] N. W. Ashcroft and N. D. Mermin, *Solid State Physics* (Saunders College, Philadelphia, 1976).
[11] I. P. Morton and M. F. Lewis, Phys. Rev. B **3**, 552 (1971).
[12] L. J. Challis, A. M. deGoer, K. Guckelsberger, and G. A. Slack, Proc. R. Soc. London, Ser. A **330**, 29 (1972).
[13] H. M. Rosenberg and B. Sujak, Philos. Mag. **5**, 1299 (1960).
[14] Neelmani and G. S. Verma, Phys. Rev. B **6**, 3509 (1972).
[15] W. Low and M. Weger, Phys. Rev. **118**, 1119 (1960).
[16] A. Hjorstberg, B. Nygren, and J. T. Vallin, Solid State Commun. **16**, 105 (1975).
[17] L. A. Turk and P. G. Klemens, Phys. Rev. B **9**, 4422 (1974).